SUPPORTING INFORMATION

Optical memory effect in a dynamic gadolinium–tetracyanidoplatinate coordination polymer for sensing deviations in temperature and humidity

Maciej Wyczesany,[ab] Michał Heczko,[a] Mateusz Reczyński,[a] Barbara Sieklucka,[a] and Szymon Chorazy*[a]

[a]Faculty of Chemistry, Jagiellonian University, Gronostajowa 2, 30-387 Krakow, Poland

[b]Doctoral School of Exact and Natural Sciences, Jagiellonian University, Łojasiewicza 11, 30-348 Kraków, Poland.

*Corresponding author: simon.chorazy@uj.edu.pl

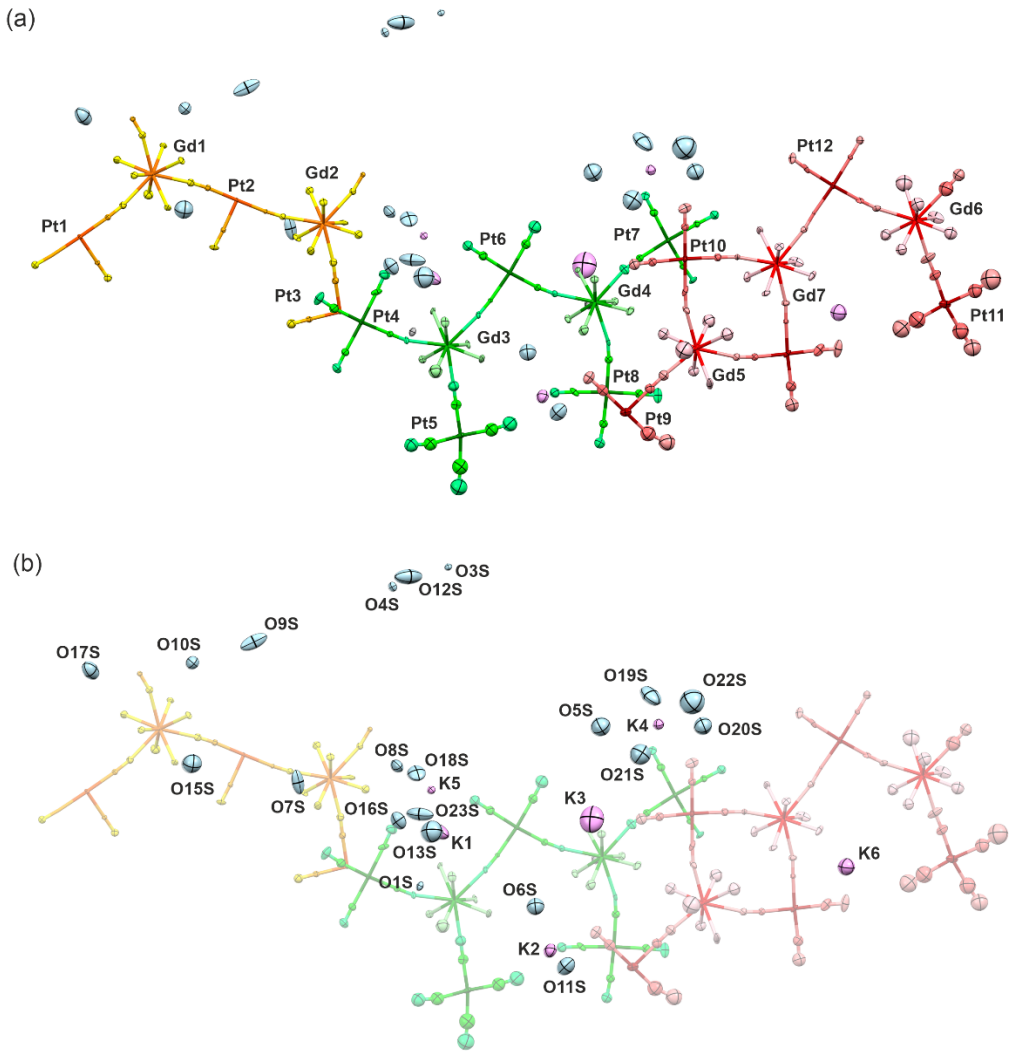

Fig. S1 The asymmetric unit of $\mathbf{1}^{\mathbf{MS}}$ with the atoms labeling schemes: (a) labeling scheme for all Gd and Pt centers, (b) labeling scheme for K^+ ions and O-atoms of uncoordinated water molecules. Thermal ellipsoids are presented at the 50% probability level. The related bond lengths and angles are collected in Tables S2 and S3 (Part 1 of 2).

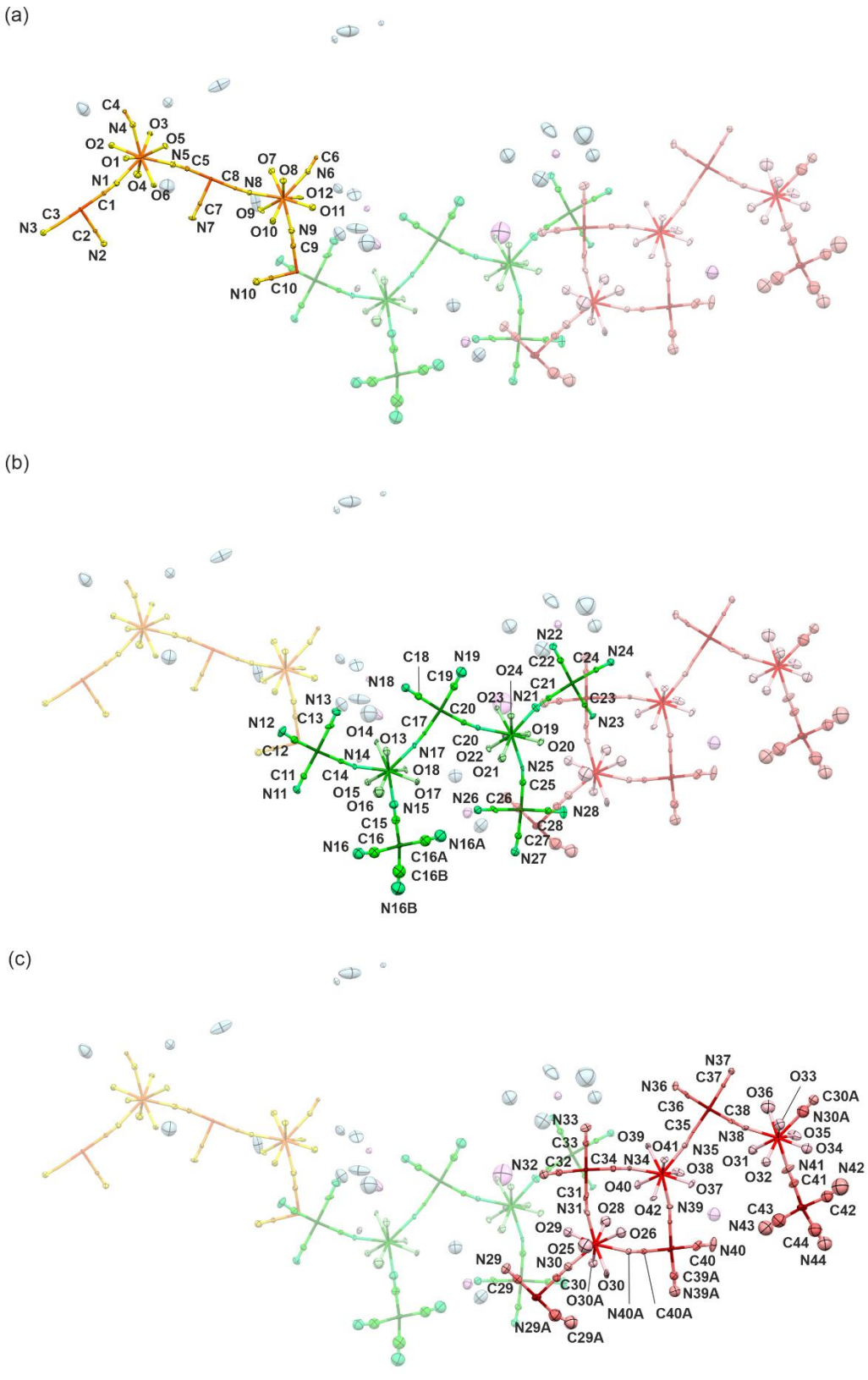

Fig. S1 The asymmetric unit of $\mathbf{1}^{MS}$ with the atoms labeling schemes: (a) labeling scheme for non-hydrogen atoms of layered coordination component (see Fig. 1) of the material, (b) labeling scheme for non-hydrogen atoms of molecule-based coordination components (see Fig. 1) of the material, (c) labeling schem for non-hydrogen atoms of chain coordination component (see Fig. 1) of the materials. Thermal ellipsoids are presented at the 50% probability level. The related bond lengths and angles are collected in Tables S2 and S3 (Part 2 of 2).

Table S1 Crystal data and structure refinement for $\mathbf{1^{MS}}$.

method		single-crystal XRD
formula		$C_{100}H_{230}Gd_{14}K_8N_{100}O_{128}Pt_{25}$
formula weight [g·mol^{-1}]		12273.38
T [K]		100(2)
λ [Å]		0.71075
crystal system		Triclinic
space group		*P -1*
unit cell	a [Å]	16.4805(13)
	b [Å]	17.7790(14)
	c [Å]	26.070(2)
	α [deg]	109.461(3)
	β [deg]	91.587(3)
	γ [deg]	91.105(3)
V [Å^3]		7196.3(10)
Z		1
calculated density [g·cm^{-3}]		2.832
absorption coefficient [cm^{-1}]		15.48
F(000)		5552
crystal size [mm × mm × mm]		0.3 × 0.15 × 0.1
crystal description		green block
θ range [deg]		2.129- 25.027
limiting indices		-19 < h < 19 -21 < k < 21 -31 < l < 30
collected reflections		104727
unique reflections		5973
R_{int}		0.0835
completeness [%]		99.8
data/restraints/parameters		25386/811/2053
GOF on F^2		1.124
final R indices		R_1 = 0.0835 [$I > 2\sigma(I)$] wR_2 = 0.1143 (all)
largest diff peak/hole [e·Å^{-3}]		4.912/-6.585

Table S2 Detailed metric parameters of gadolinium(III) complexes in $\mathbf{1}^{MS}$ (Part 1 of 2).

Parameter	Distance / Å
Gd1-O1	2.41(1)
Gd1-O2	2.44(2)
Gd1-O3	2.43(1)
Gd1-O4	2.43(1)
Gd1-O5	2.45(1)
Gd1-O6	2.44(2)
Gd1-N1	2.54(1)
Gd1-N4	2.54(2)
Gd1-N5	2.52(2)
Gd2-O7	2.38(1)
Gd2-O8	2.46(1)
Gd2-O9	2.44(1)
Gd2-O10	2.47(1)
Gd2-O11	2.44(1)
Gd2-O12	2.43(1)
Gd2-N6	2.57(1)
Gd2-N8	2.58(1)
Gd2-N9	2.46(2)
Gd3-O13	2.41(2)
Gd3-O14	2.42(1)
Gd3-O15	2.50(1)
Gd3-O16	2.50(2)
Gd3-O17	2.44(1)
Gd3-O18	2.39(1)
Gd3-N14	2.53(2)
Gd3-N15	2.50(2)
Gd3-N17	2.57(1)
Gd4-O19	2.44(1)
Gd4-O20	2.49(2)
Gd4-O21	2.43(1)
Gd4-O22	2.38(1)
G4-O23	2.47(1)
Gd4-O24	2.40(1)
Gd4-N20	2.60(2)
Gd4-N21	2.59(1)
Gd4-N25	2.55(2)

Table S2 Detailed metric parameters of gadolinium(III) complexes in $\mathbf{1}^{MS}$ (Part 2 of 2).

Parameter	Distance / Å
Gd5-O25	2.44(3)
Gd5-O26	2.49(2)
Gd5-O28	2.39(2)
Gd5-O29	2.42(2)
Gd5-O30	2.39(2)
Gd5-O30A	2.41(2)
Gd5-N30	2.39(2)
Gd5-N31	2.52(2)
Gd5-N40A	2.58(2)
Gd6-O31	2.44(2)
Gd6-O32	2.39(2)
Gd6-O33	2.39(2)
Gd6-O34	2.50(2)
Gd6-O35	2.46(2)
Gd6-O36	2.48(3)
Gd6-N30A	2.58(2)
Gd6-N38	2.56(2)
Gd6-N41	2.54(2)
Gd7-O37	2.39(2)
Gd7-O38	2.44(2)
Gd7-O39	2.40(2)
Gd7-O40	2.45(1)
Gd7-O41	2.48(1)
Gd7-O42	2.41(1)
Gd7-N34	2.51(2)
Gd7-N35	2.61(1)
Gd7-N39	2.57(2)

Table S3 Detailed metric parameters of tetracyanidoplatinate(II) complexes in $\mathbf{1}^{MS}$ (Part 1 of 2).

Parameter	Distance / Å
Pt1-C1	2.012(17)
Pt1-C2	1.966(16)
Pt1-C3	2.011(14)
Pt1-C4	1.985(16)
Pt2-C5	2.011(17)
Pt2-C6	1.968(16)
Pt2-C7	1.973(16)
Pt2-C8	1.956(15)
Pt3-C9	1.971(18)
Pt3-C10	1.989(17)
Pt4-C11	2.04(2)
Pt4-C12	1.96(2)
Pt4-C13	1.99(2)
Pt4-C14	1.988(18)
Pt5-C15	1.93(2)
Pt5-C16	1.92(3)
Pt5-C16A	1.93(3)
Pt5-C116B	1.91(4)
Pt6-C17	2.001(16)
Pt6-C18	1.96(2)
Pt6-C19	1.95(2)
Pt6-C20	2.006(18)
Pt7-C21	1.987(19)
Pt7-C22	1.971(19)
Pt7-C23	1.988(18)
Pt7-C24	1.967(18)
Pt8-C25	2.02(2)
Pt8-C26	1.95(2)
Pt8-C27	1.95(2)
Pt8-C28	1.96(2)
Pt9-C29	1.98(2)
Pt9-C29A	1.96(4)
Pt9-C30	2.00(2)
Pt9-C2A	1.94(3)
Pt10-C31	1.99(2)
Pt10-C32	2.01(2)
Pt10-C33	1.966(19)
Pt10-C34	1.985(19)

Table S3 Detailed metric parameters of tetracyanidoplatinate(II) complexes in $\mathbf{1}^{MS}$ (Part 2 of 2).

Parameter	Distance / Å
Pt11-C41	1.91(2)
Pt11-C42	1.99(3)
Pt11-C43	1.922(18)
Pt11-C44	1.975(18)
Pt12-C35	2.006(15)
Pt12-C36	2.04(2)
Pt12-C37	1.975(17)
Pt12-C38	1.961(18)
Pt13-C39	1.991(17)
Pt13-C39A	1.98(2)
Pt13-C40	1.95(3)
Pt13-C40A	2.008(18)
Pt3-Pt4	3.247
Pt7-Pt10	3.356
Pt8-Pt9	3.327
Pt10-Pt12	3.306

Table S4 Results of Continuous Shape Measure Analysis for $[Gd^{III}(H_2O)_6(NC)_3]$ complexes in the crystal structure of $\mathbf{1}^{\mathbf{MS}}$.[S1,S2]

Gd center	CSM parameters*				geometry
	JTCTPR-9	CSAPR-9	TCTPR-9	JCSAPR-9	
Gd1	1.569	0.922	**0.321**	1.763	**TCTPR-9**
Gd2	1.621	0.746	**0.301**	1.529	**TCTPR-9**
Gd3	2.185	**0.229**	0.910	0.961	**CSAPR-9**
Gd4	1.417	**0.761**	1.401	**0.504**	**JCSAPR-9/CSAPR-9**
Gd5	0.927	**0.189**	2.179	0.928	**CSAPR-9**
Gd6	1.704	**0.925**	1.702	**0.851**	**JCSAPR-9/CSAPR-9**
Gd7	1.521	**0.774**	1.465	**0.499**	**JCSAPR-9/CSAPR-9**

* CSM parameters:

CSM CSAPR-9 = the parameter related to the spherical capped square antiprism (C_{4v} symmetry)

CSM TCTPR-9 = the parameter related to the spherical tricapped trigonal prism (D_{3h} symmetry)

CSM JCSAPR-9 = the parameter related to the capped square antiprism (C_{4v} symmetry)

CSM JTCTPR-9 = the parameter related to the tricapped trigonal prism J51 (D_{3h} symmetry)

CSM = 0 for the ideal geometry and the increase of CSM parameter corresponds to the increasing distortion from the ideal polyhedron.

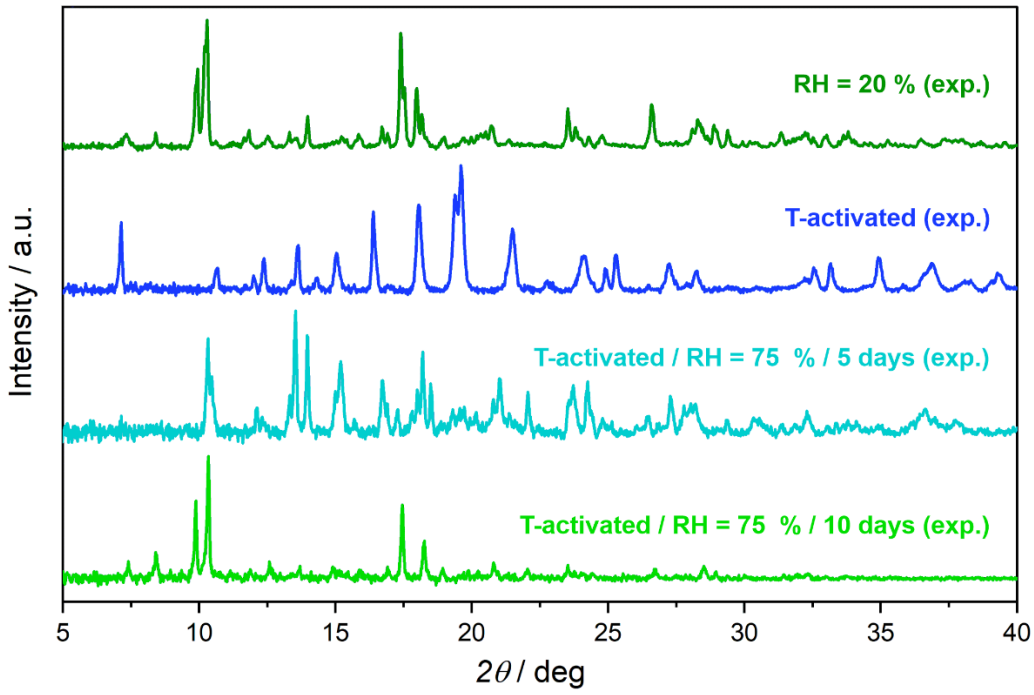

Fig. S2 Experimental powder X-ray diffraction (P-XRD) patterns of $\mathbf{1}^{\mathbf{H2(20\%)}}$ (see Fig. 5) compared with P-XRD patterns obtained for the temperature-activated sample (by heating to 150 °C) right after thermal treatment, as well as after 5 and 10 days of subsequent stabilization in RH = 75%. It is important to note here that the attempts to index the obtained P-XRD patterns have been made using the EXPO2014 software.[S3] Unfortunately, these trials were unsuccessful. It is probably caused by the fact that the initial phase crystallizes in the low-symmetry *P*-1 space group within the large unit cell volume, which combined with a large number of heavy atoms in the unit cell leads to a complex P-XRD pattern with a large number of closely lying peaks (which can be also seen on the diffractograms of other phases). Additionally, on all of the P-XRD patterns, we observe relatively high background and low data quality. This is partly due to the strong X-ray absorption by heavy metals and partly because of the texture effect. The latter may occur since **1** crystallizes as long needle-shaped crystals, which might align along the capillary's rotation axis.

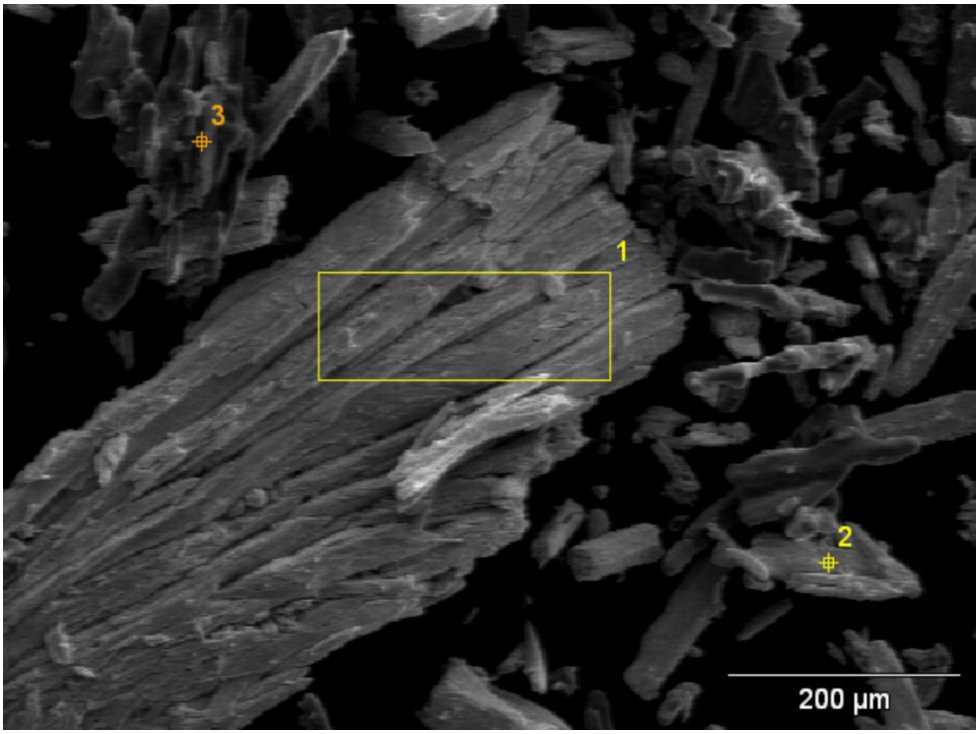

Fig. S3 The SEM image of the microcrystalline sample of $\mathbf{1}^{\mathbf{H2}}$ (see Fig. 5) with the labeling of points 2 and 3 as well as area 4 targeted for the ED-XMA experiment. Analyses were performed on several crystallites to confirm the homogeneous metal composition of the whole sample.

Comment on Fig. S3:

ED-XMA (energy dispersive X-ray microanalysis) analysis was conducted on a number of different single crystals and a few areas on a selected single crystal. The results of atomic compositions of Gd and Pt metal centers were averaged. The obtained average atomic compositions were used to estimate the relative metal composition. It was calculated assuming 25 Pt centers for the formula of the compound, according to the crystal structures (Fig. 1 and Table S1). These proposed metal compositions were used to determine the full formula of the respective compounds, taking into account the results of CHN elemental analyses (see Experimental Section). The identical methodology was previously used by us for heterometallic cyanido-bridged coordination clusters and chains.[S4,S5] From this analysis, it was found that for each set of 25 Pt centers one can count 8 K and 14 Gd metal centers.

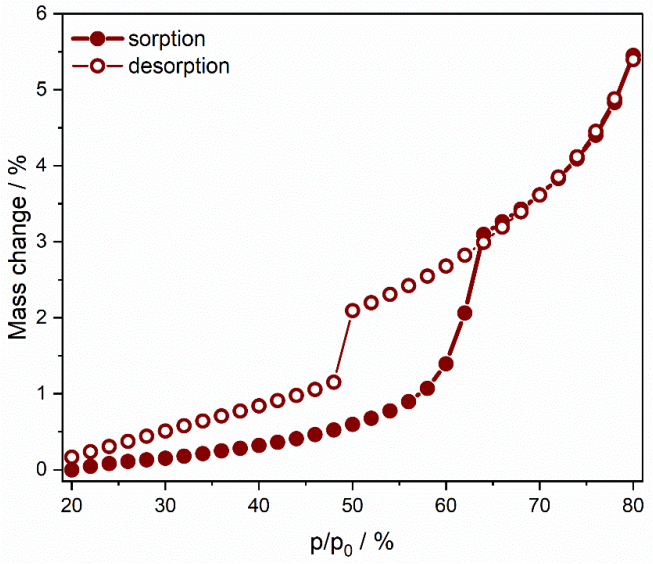

Fig. S4 Mass change versus partial pressure of water dependence for **1** gathered in the limited 20–80% relative humidity (RH) range.

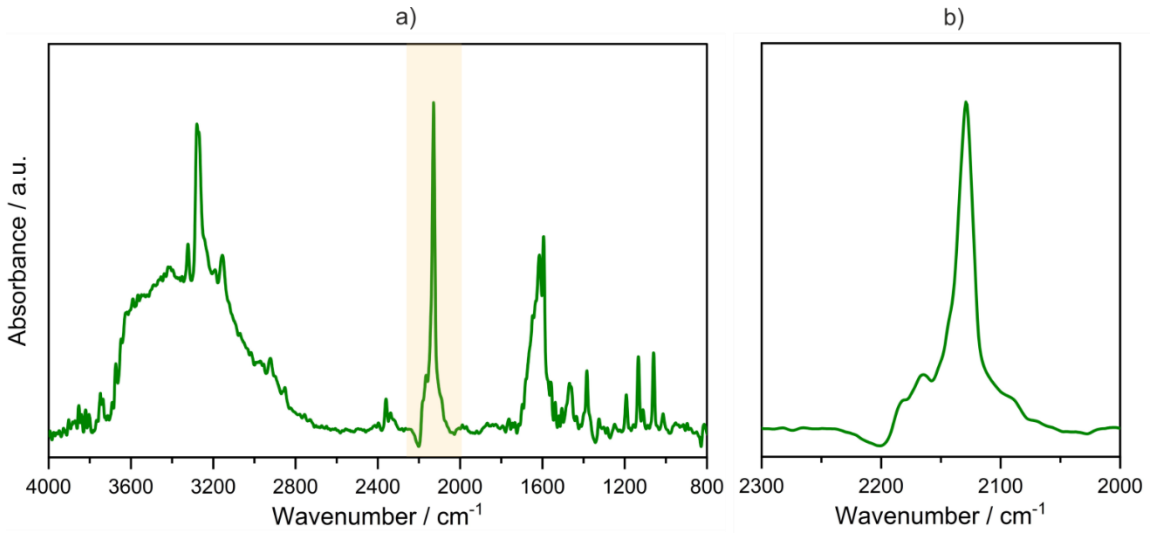

Fig. S5 The infrared (IR) absorption spectrum of the selected crystalline object of $\mathbf{1^{H2}}$: (a) presented for the broad 4000-800 cm^{-1} range and (b) the limited 2300-2000 cm^{-1} range corresponding to the stretching vibrations of cyanido ligands.[S6,S7] Note that the spectrum was measured on the crystalline object but it was not a well-shaped single crystal as the crystals of 1MS (crystals covered by a mother solution) lost the good quality upon the exposition to the air atmosphere. It can be illustrated by their shape and texture presented on the SEM image (Fig. S3).

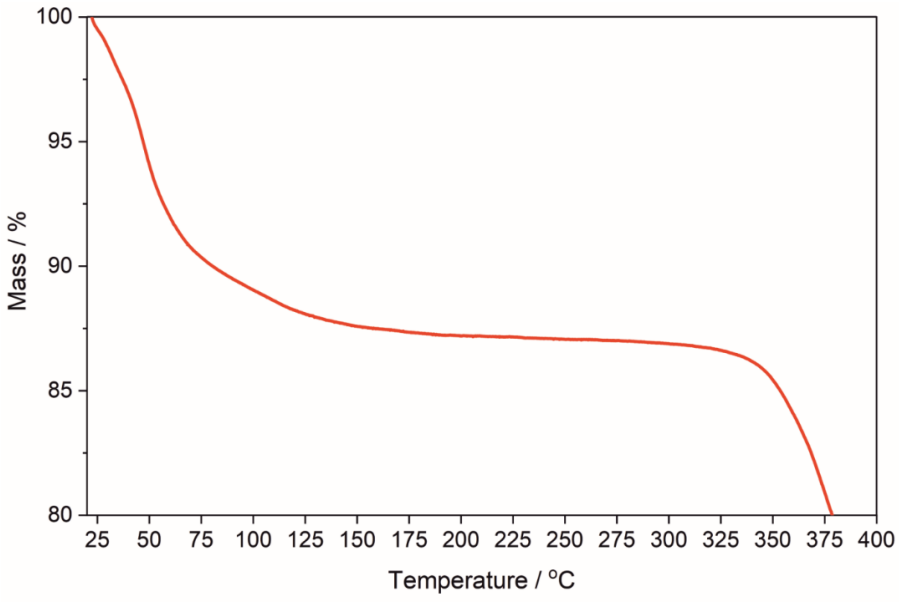

Fig. S6 The thermogravimetric (TG) curve collected in the temperature range of 20–370 °C for the sample of **1** stabilized in the RH = 20% before measurement.

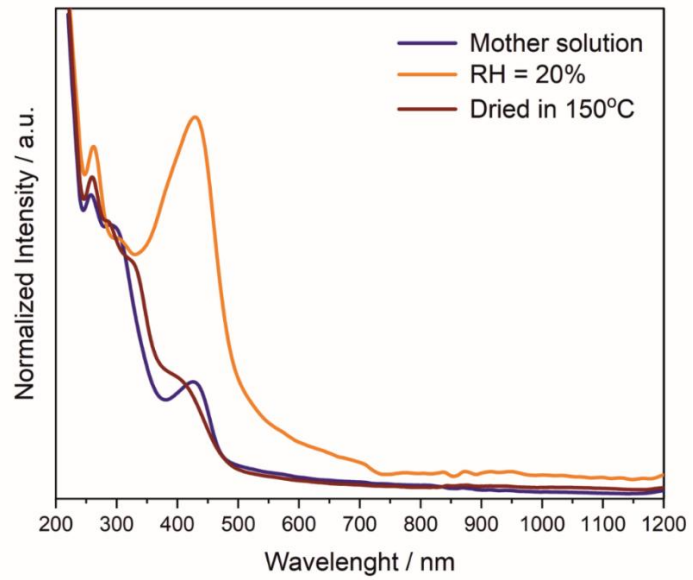

Fig. S7 UV-vis-NIR solid-state absorption spectra of the polycrystalline sample of **1,** measured directly after picking them from the mother solution (Mother solution, dark blue), as well as stabilized in 20% of relative humidity (RH = 20%, orange) and dried at 150 °C for 1h (Dried in 150°C, purple).

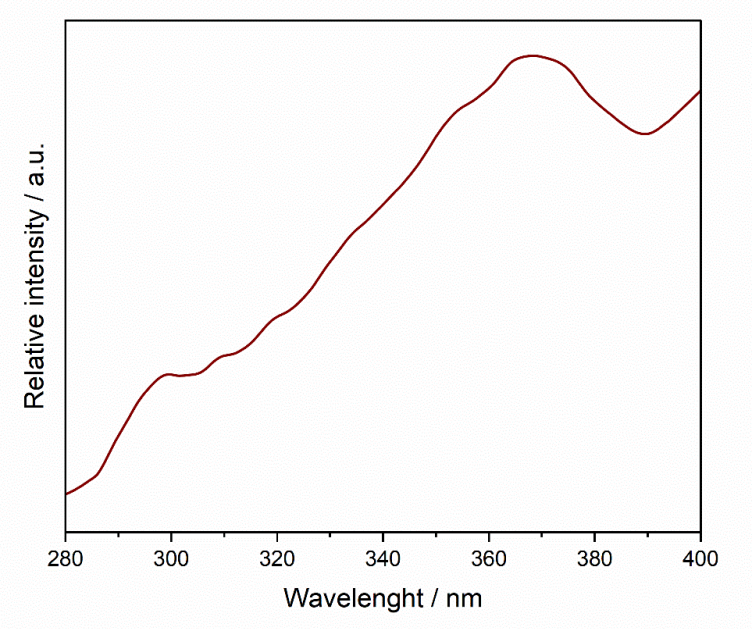

Fig. S8 The room-temperature excitation spectrum of $\mathbf{1}^{\mathbf{H2(20\%)}}$ (see Fig. 5) for the emission maximum at 535 nm.

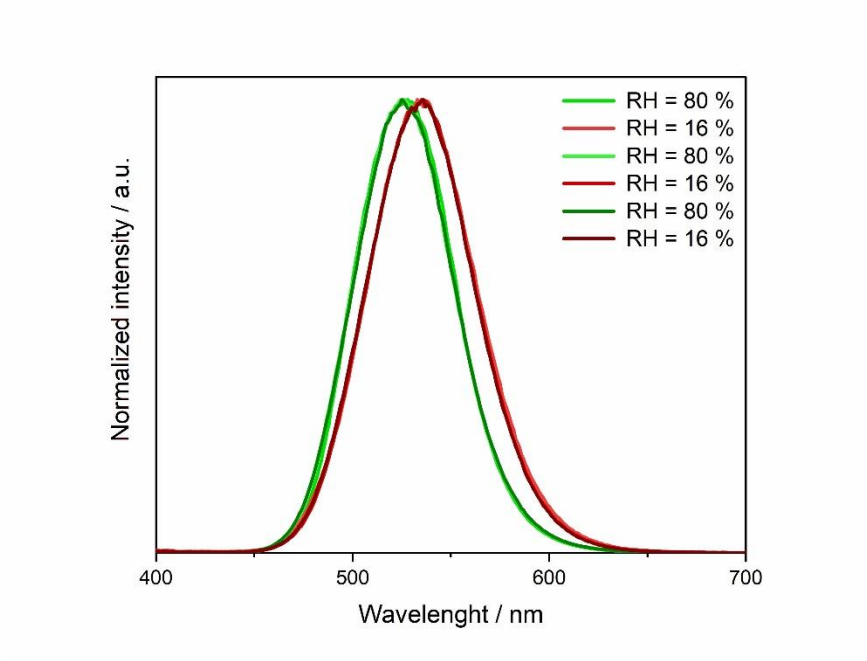

Fig. S9 Emission spectra under 350 nm excitation upon cycling between 16% (phase named $\mathbf{1}^{\mathbf{H2}}$, see Fig. 5) and 80% (phase named $\mathbf{1}^{\mathbf{H1}}$) of relative humidity.

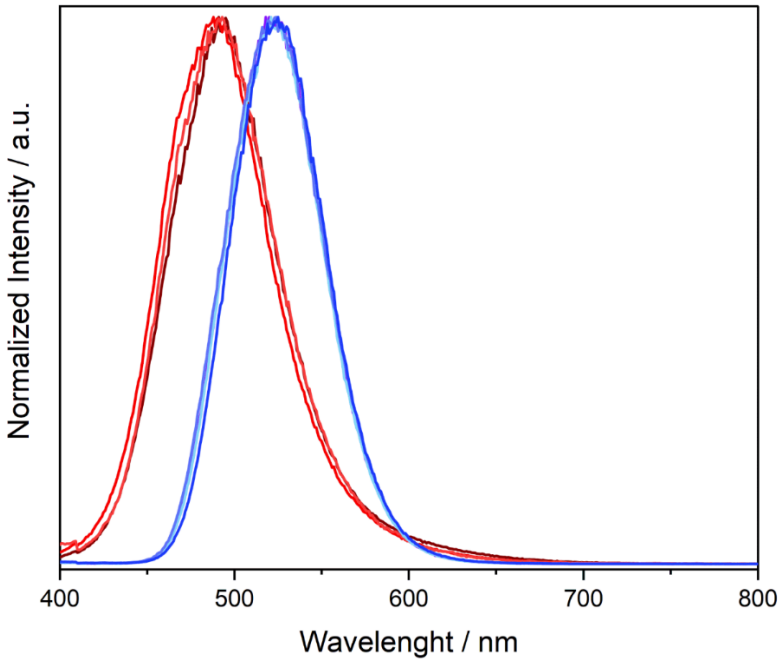

Fig. S10 Emission spectra under 350 nm excitation upon cycling between thermal activation at 150°C (red) and the further stabilization of the material in RH = 75% at room temperature (blue).

References to Supporting Information

(S1) M. Llunell, D. Casanova, J. Cirera, J. Bofill, P. Alemany, S. Alvarez, M. Pinsky and D. Avnir, *SHAPE v. 2.1, Program for the Calculation of Continuous Shape Measures of Polygonal and Polyhedral Molecular Fragments*; University of Barcelona: Barcelona, 2013.

(S2) D. Casanova, J. Cirera, M. Llunell, P. Alemany, D. Avnir and S. Alvarez, *J. Am. Chem. Soc*., 2004, **126**, 1755–1763.

(S3) A. Altomare, C. Cuocci, C. Giacovazzo, A. Moliterni, R. Rizzi, N. Corriero and A. Falcicchio, *J. Appl. Cryst.*, 2013, **46**, 1231–1235.

(S4) M. Liberka, J. Kobylarczyk, T. M. Muziol, S. Ohkoshi, S. Chorazy and R. Podgajny, *Inorg. Chem. Front*., 2019, **6**, 3104–3118.

(S5) M. Wyczesany, J. J. Zakrzewski, B. Sieklucka and S. Chorazy, *J. Mater. Chem. C*, 2022, **10**, 12054–12069.

(S6) B. A. Maynard, P. A. Smith, L. Ladner, A. Jaleel, N. Beedoe, C. Crawford, Z. Assefa and R. E. Sykora, *Inorg. Chem*., 2009, **48**, 6425–6435.

(S7) P. A. Smith, C. Crawford, N. Beedoe, Z. Assefa and R. E. Sykora, *Inorg. Chem*., 2012, **51**, 12230–12241.